ISSN 1070-3632, Russian Journal of General Chemistry, 2007, Vol. 77, No. 4, pp. 517–523. © Pleiades Publishing, Ltd., 2007.
Original Russian Text © I.A. Zvereva, A.G. Cherepova, Yu.E. Smirnov, 2007, published in Zhurnal Obshchei Khimii, 2007, Vol. 77, No. 4, pp. 557–563.

Cation Distribution and Interatomic Interactions in Oxides with Heterovalent Isomorphism: XII.[1] $Gd_2Sr_{1-x}Ca_xAl_2O_7$ Solid Solutions

I. A. Zvereva, A. G. Cherepova, and Yu. E. Smirnov

St. Petersburg State University,
Universitetskii pr. 26, St. Petersburg, 198504 Russia

Received October 5, 2006

Abstract — The area of existence of $Gd_2Sr_{1-x}Ca_xAl_2O_7$ solid solutions at $x \le 0.5$ was determined by the X-ray phase analysis. It was found by full-profile X-ray structural analysis that, in contrast to $La_2Sr_{1-x}Ca_x \cdot Al_2O_7$ solid solutions, the Ca^{2+} cations occupy not only AO_9 nine-vertex fragments, but also AO_{12} oxygen cubooctahedra. Full ordering of Sr^{2+} cations in the perovskite layer is observed at the calcium content x 0.5.
DOI: 10.1134/S1070363207040444

To examine common regular trends in the effect of cationic substitution on the stability of perovskite-like layered structures in complex oxides, we perform crystalchemical studies of the $Ca^{2+} \to Sr^{2+}$ substitution in $Ln_2SrAl_2O_7$ matrixes.

The $Ca^{2+} \to Sr^{2+}$ substitution in perovskite-like layered oxides has been studied in superconducting cuprates $La_{2-x}Sr(Ca)_xCu_2O_{6-\delta}$ [2, 3] and in manganites with enormous magnetoresistance $La_{1.2}(Sr_{1-x}Ca_x)_{1.8} \cdot Mn_2O_7$ and $La_{1.4}(Sr_{1-x}Ca_x)_{1.6}Mn_2O_7$ [4, 5]. As a result, it was found that the critical temperatures decrease as the concentration of calcium increases and that solid solutions become heterogeneous. Crystal-chemical effects of such substitution are close to the modifications detected in perovskite-like layered aluminates and aluminochromites $LnSr(Ca)Al_{1-x}Cr_xO_4$ [6]. The most essential fact is the destabilizing role of Ca^{2+} atoms: initially metastable $LaCaAlO_4$ completely disintegrates into structurally related phases $LaAlO_3$ and CaO. The reason is rather complicated crystal-chemical mechanism caused by the ordering of Ca^{2+} and La^{3+} atoms. It was found recently that cationic ordering in $La_2Sr_{1-x}Ca_xAl_2O_7$ [7] and $Nd_2Sr_{1-x}Ca_xAl_2O_7$ solid solutions [8] restrics the area of existence of solid solutions.

Here we report on a crystal-chemical study of solid solutions of isomorphous isovalent substitution of calcium atoms for strontium atoms in a $Gd_2SrAl_2O_7$ matrix and compare the data found for $Gd_2Sr_{1-x}Ca_x \cdot Al_2O_7$ solutions and for previously studied $La_2Sr_{1-x}Ca_xAl_2O_7$ and $Nd_2Sr_{1-x}Ca_xAl_2O_7$ solutions, namely, the distributions of Ca^{2+}, Sr^{2+}, and Ln^{3+} atoms over two nonequivalent positions and the chemical bond anisotropy in coordination polyhedra depending on the composition of $Ln_2Sr_{1-x}Ca_xAl_2O_7$ solid solutions.

The complex aluminate $Gd_2SrAl_2O_7$ crystallizing in the $Sr_3Ti_2O_7$ structural type (space group *I*4/*mmm*) belongs to Ruddlesden–Popper phases [9]. It is built by a block principle from interpenetrating fragments of perovskite (*P*) and rock salt (*RS*) structures with the layer sequence ...(*P*)(*P*)(*RS*)(*P*)(*P*)(*RS*)... (Fig. 1a). In such structures, isomorphous cations Gd^{3+} and Sr^{2+} occupy two common structural positions 2b and 4e, the centers of oxygen polyhedra with coordination numbers 12 (AO_{12} cuboctahedra) and 9 (monocapped distorted tetragonal antiprisms AO_9) (Fig. 1b). According to the common interpretation, the first of them is in the double perovskite layers (*P*)(*P*), and the second, in (*RS*) layers.

The area of existence of single-phase solid solutions $Gd_2Sr_{1-x}Ca_xAl_2O_7$ ($x \le 0.5$) was determined by X-ray phase analysis. In this area, only reflections of the $Sr_3Ti_2O_7$ structure are present in the X-ray patterns (Fig. 2). For the solid solution with $x > 0.5$, in addition to reflections of the $Sr_3Ti_2O_7$ structure, there are reflections of other phases: $Gd_2Sr_{1-x}Ca_xAl_2O_7$ solid solution and $GdCaAlO_4$ (K_2NiF_4 structural type, *P*/*RS* junction). It follows from the X-ray pattern that the $Nd_2Sr_{0.5}Ca_{0.5}Al_2O_7$ solid solution, and also $NdCaAlO_4$ and $NdAlO_3$ (perovskite structural type) are formed in the case of neodymium solid solutions at $0.5 < x < 1$. In the case of lanthanum, the known thermal instability of the oxides $LaCaAlO_4$ and $La_2SrAl_2O_7$

[1] For communication XI, see [1].

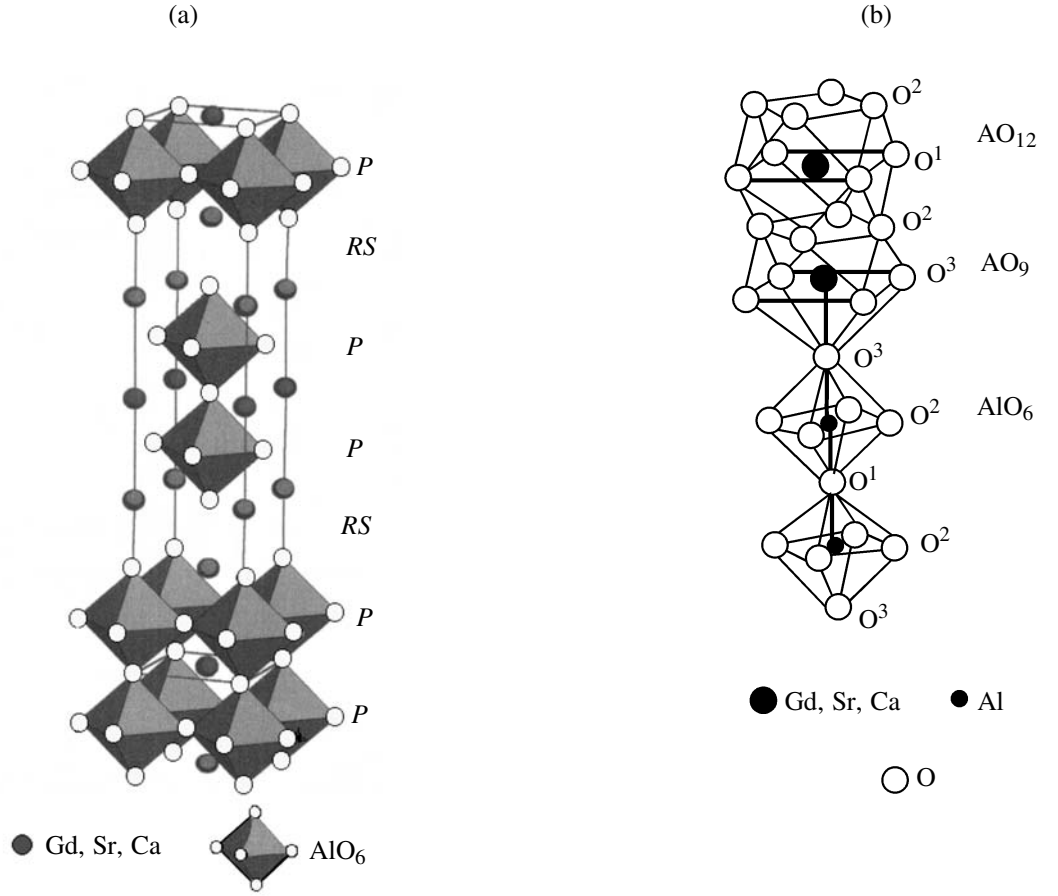

Fig. 1. Crystal structure of the $Gd_2SrAl_2O_7$ and of $Gd_2Sr_{1-x}Ca_xAl_2O_7$ solid solutions: (a) unit cell and (b) coordination polyhedra AlO_6, AO_9, and AO_{12}.

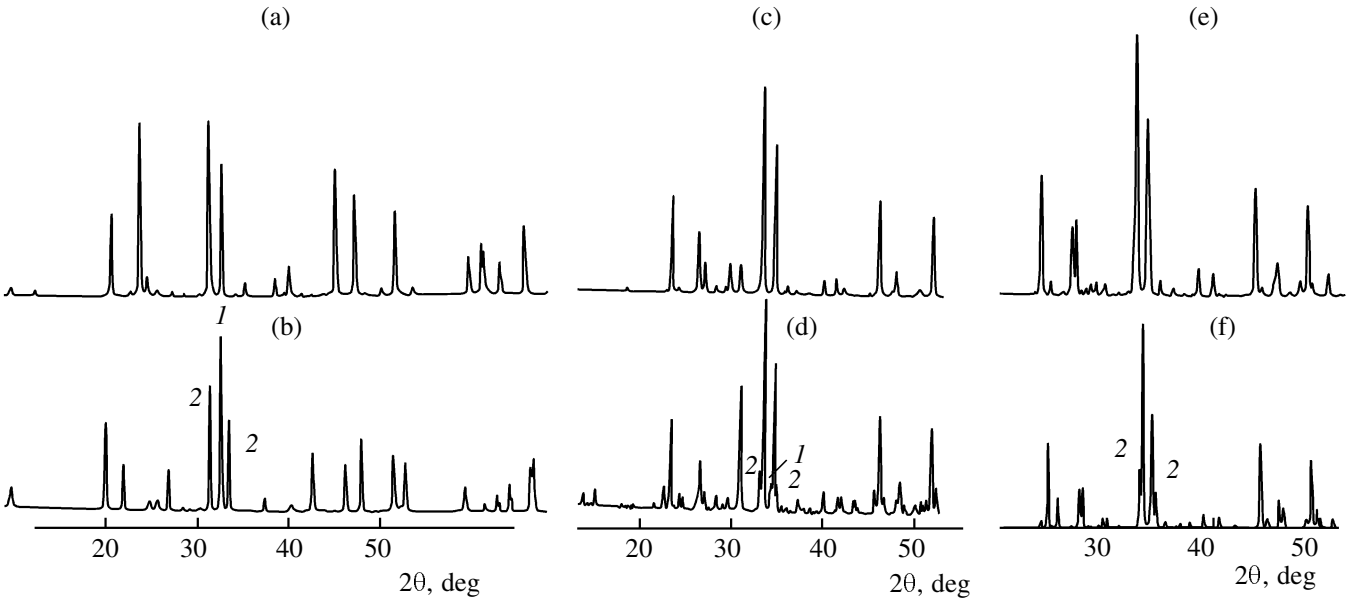

Fig. 2. X-ray diffraction patterns of solid solutions $La_2Sr_{1-x}Ca_xAl_2O_7$ [(a) $x \le 0.5$, (b) $x > 0.5$], $Nd_2Sr_{1-x}Ca_xAl_2O_7$ [(c) $x \le 0.5$, (d) $x > 0.5$] after calcination for 100 h at 1450°C, and $Gd_2Sr_{1-x}Ca_xAl_2O_7$ [(e) x 0.5, (f) x 0.7)] after calcination for 100 h at 1500°C. (*1, 2*) Main reflections of $LnAlO_3$ phase with the perovskite structure and of $LnSr_{1-x}Ca_xAlO_4$ with the K_2NiF_4-type structure.

Table 1. Parameters a and c (Å), unit cell volume V (Å^3), coordinates of atoms (x, y, z), thermal parameters B (Å^2), and structural (R_F) and profile (R_P) divergence factors (%) for $Gd_2Sr_{1-x}Ca_xAl_2O_7$ solid solutions

Atom, structural position, coordinates	Parameter	Ca content, x		
		$x = 0$	$x = 0.3$	$x = 0.5$
	a	3.7052	3.7011	3.6999
	c	19.781	19.666	19.574
	V	271.56	269.39	267.95
Gd, Sr, Ca	B	0.37 (3)	1.0 (1)	0.65 (7)
2b (0, 0, 1/2)				
Gd, Sr, Ca	z	0.3186 (2)	0.3182 (2)	0.3181 (1)
4e (0, 0, z)	B	0.37 (1)	0.23 (3)	0.34 (6)
Al	z	0.0941 (4)	0.0934 (5)	0.0946 (6)
4e (0, 0, z)	B	0.32 (3)	0.59 (8)	0.48 (6)
O^1	B	2.3 (1)	0.97 (7)	1.42 (7)
2a (0, 0, 0)				
O^2	z	0.1006 (5)	0.1007 (4)	0.1003 (4)
8g (0, 1/2, z)	B	0.65 (2)	1.13 (3)	0.99 (5)
O^3	z	0.2035 (7)	0.2007 (4)	0.2007 (5)
4e (0, 0, z)	B	0.42 (5)	3.56(6)	3.70 (5)
	R_F	3.8	4.8	4.3
	R_P	5.8	4.1	3.1

results in the fact that the products of the solid-phase reaction are $LaSr_{1-x}Ca_xAlO_4$ solid solutions and $LaAlO_3$. The limit (x 0.5) of the existence of $Gd_2Sr_{1-x}\cdot Ca_xAl_2O_7$ solid solutions coincides with the limit for $La_2Sr_{1-x}Ca_xAl_2O_7$ and $Nd_2Sr_{1-x}Ca_xAl_2O_7$ [7, 8].

Using full-profile X-ray structural analysis with subsequent refinement of structural parameters, we obtained crystal-chemical data for a series of $Gd_2Sr_{1-x}\cdot Ca_xAl_2O_7$ solid solutions, including also the population of various polyhedra by gadolinium, strontium, and calcium atoms. The calculated data are given in Tables 1 and 2.

The unit cell parameters of the $Gd_2Sr_{1-x}Ca_xAl_2O_7$ solid solution decrease as the Ca content increases (Fig. 3), which is caused by a decrease in the mean ionic radius of alkaline-earth cations (Table 3). The unit cell volume also monotonically decreases. The linear dependence of the parameter c on the composition indicates that Vegard's rule in this case is fulfilled, which confirms the formation of solid solutions. However, the dependence of parameter a on the composition deviates from linearity. This is caused by the fact that parameter a is determined by the framework of AlO_6 octahedra sharing common vertices. There is a compression limit for the octahedra and, hence, a limit for a decrease in parameter a. That is the reason why, starting from a certain Ca concentration, the decrease in parameter a decelerates. It is probably a common feature of strongly anisotropic structures (in this case, parameter c is greater than parameter a by a factor of 5). Current coordinates of atoms in fractions of the lattice periods vary only slightly. The strongest variations are observed for O^3 oxygen atoms (Table 1).

The results of studying the distribution of cations over structural positions (Table 2) are given in comparison with the data for oxides $Ln_2SrAl_2O_7$ (Ln = La, Nd, Gd) and solid solutions $La_2Sr_{1-x}Ca_xAl_2O_7$ and $Nd_2Sr_{1-x}Ca_xAl_2O_7$. It was found that in the solid solutions, as well as in $Gd_2SrAl_2O_7$, gadolinium atoms preferentially occupy AO_9 antiprisms located in *RS* layers. However, as the calcium content in-

Table 2. Parameters of occupation of AO_{12} cuboctahedra and AO_9 antiprisms by isomorphous cations in $Ln_2SrAl_2O_7$ and in $Ln_2Sr_{0.5}Ca_{0.5}Al_2O_7$ solid solutions

Oxide, solid solution	AO_{12} cuboctahedron			AO_9 antiprism		
	Ln^{3+}	Sr^{2+}	Ca^{2+}	Ln^{3+}	Sr^{2+}	Ca^{2+}
	Random distribution					
$Ln_2SrAl_2O_7$	0.67	0.33		1.33	0.67	
$Ln_2Sr_{0.5}Ca_{0.5}Al_2O_7$	0.67	0.16	0.16	1.33	0.33	0.33
	Calculated data					
$Nd_2SrAl_2O_7$	0.54	0.46		1.46	0.54	
$Nd_2Sr_{0.5}Ca_{0.5}Al_2O_7$	0.66	0.20	0.14	1.34	0.30	0.36
$La_2SrAl_2O_7$	0.73	0.27		1.27	0.73	
$La_2Sr_{0.5}Ca_{0.5}Al_2O_7$	0.67	0.33	0	1.33	0.17	0.50
$Gd_2SrAl_2O_7$	0.28	0.72		1.72	0.28	
$Gd_2Sr_{0.5}Ca_{0.5}Al_2O_7$	0.38	0.5	0.12	1.62	0	0.38

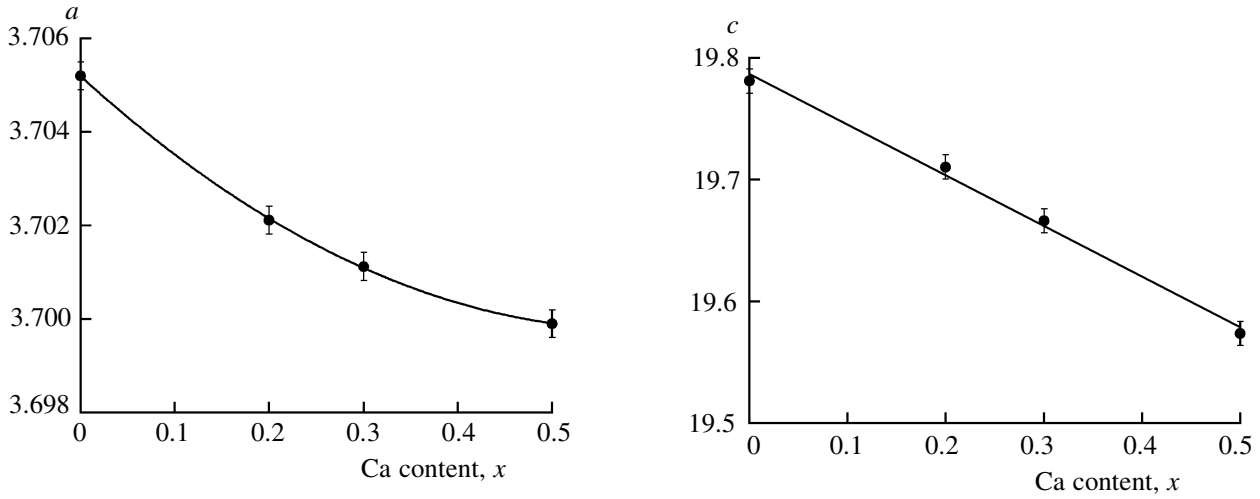

Fig. 3. Unit cell parameters a and c of $Gd_2Sr_{1-x}Ca_xAl_2O_7$ solid solutions as functions of calcium content.

creases, this effect of positional ordering weakens. This is due to the fact that the Gd^{3+} and Ca^{2+} cations, rather close in size, compete in occupation of smaller AO_9 antiprisms in the rock salt layer. Unlike $La_2Sr_{1-x}\cdot Ca_xAl_2O_7$ solid solutions, where calcium atoms occupy only AO_9 polyhedra, calcium cations in $Gd_2Sr_{1-x}Ca_xAl_2O_7$ solutions are distributed over two positions. The Sr^{2+} cations, which are appreciably larger than Gd^{3+} and Ca^{2+} cations, mainly occupy AO_{12} cuboctahedra in a perovskite layer. At the calcium content x 0.5, complete ordering of Sr^{2+} cations in the perovskite layer is observed.

The fact that the distribution of isomorphous atoms over two positions differs from a random distribution is attributable to the difference in the ionic radii, as smaller atoms occupy smaller AO_9 polyhedra. A similar phenomenon was already observed in $Ln_2\cdot SrAl_2O_7$ (Ln = La–Ho) [11] and in the case of the substitution of calcium for strontium in a $La_2SrAl_2O_7$ matrix [7]. In the first case, the probability of the occupation of antiprisms by lanthanides and of oxygen cuboctahedra by Sr^{2+} cations increases as the lanthanide ionic radius increases in the series La–Ho. In $La_2SrAl_2O_7$, the distribution of lanthanum and strontium atoms is the closest to random (because of the closeness of the La^{3+} and Sr^{2+} ionic radii, Table 3). In the case of $Nd_2SrAl_2O_7$ and $Gd_2SrAl_2O_7$, the occupancy of AO_{12} polyhedrons by lanthanide atoms (0.54 and 0.28, respectively) is less than the average statistical value (0.67). In $La_2Sr_{1-x}Ca_xAl_2O_7$ solid solutions, smaller calcium atoms occupy only AO_9 polyhedra. In $Gd_2Sr_{1-x}Ca_xAl_2O_7$ solutions, strontium cations, starting from a certain concentration, occupy only cuboctahedra. An intermediate situation takes place in neodymium-containing solid solutions: no ordering of isomorphous cations is observed at all, although neodymium cations to a greater extent than strontium are displaced from antiprisms into cubooctahedra. In gadolinium-containing solutions, gadolinium cations are also displaced to a greater extent into cubooctahedra by smaller calcium cations. Probably, at an insignificant size difference, a cation with a higher charge occupies a position surrounded by a larger number of oxygen anions. A similar phenomenon takes place in $La_2SrAl_2O_7$ and in the complex bismuth oxide $(Ba, K)_3Bi_2O_7$ [12]. Moreover, in the case when not two but several cations occupy equivalent positions, a disordering effect of the third "component" is observed.

Table 3. Crystal-chemical radii (Å) of cations after Shannon [10] for coordination numbers (CN) 9 and 12

Cation	CN 9	CN 12
Sr^{2+}	1.31	1.44
Ca^{2+}	1.18	1.34
Gd^{3+}	1.11	1.22
Nd^{3+}	1.16	1.27
La^{3+}	1.22	1.36

The effect of cationic ordering is manifested in a greater variation of the AO^3 bond length in the AO_9 polyhedra compared to all distances in AO_{12} (Fig. 4). The $A–O^3$ distance in $La_2Sr_{0.5}Ca_{0.5}Al_2O_7$ decreases by 0.22 Å and in $Nd_2Sr_{0.5}Ca_{0.5}Al_2O_7$, by only 0.08 Å, whereas in $Gd_2Sr_{0.5}Ca_{0.5}Al_2O_7$ it increases by 0.08 Å. In the first two solutions, the effect of positional ordering of Ca^{2+} and Sr^{2+} takes place. In the lanthanum-containing solution, much more calcium cations are

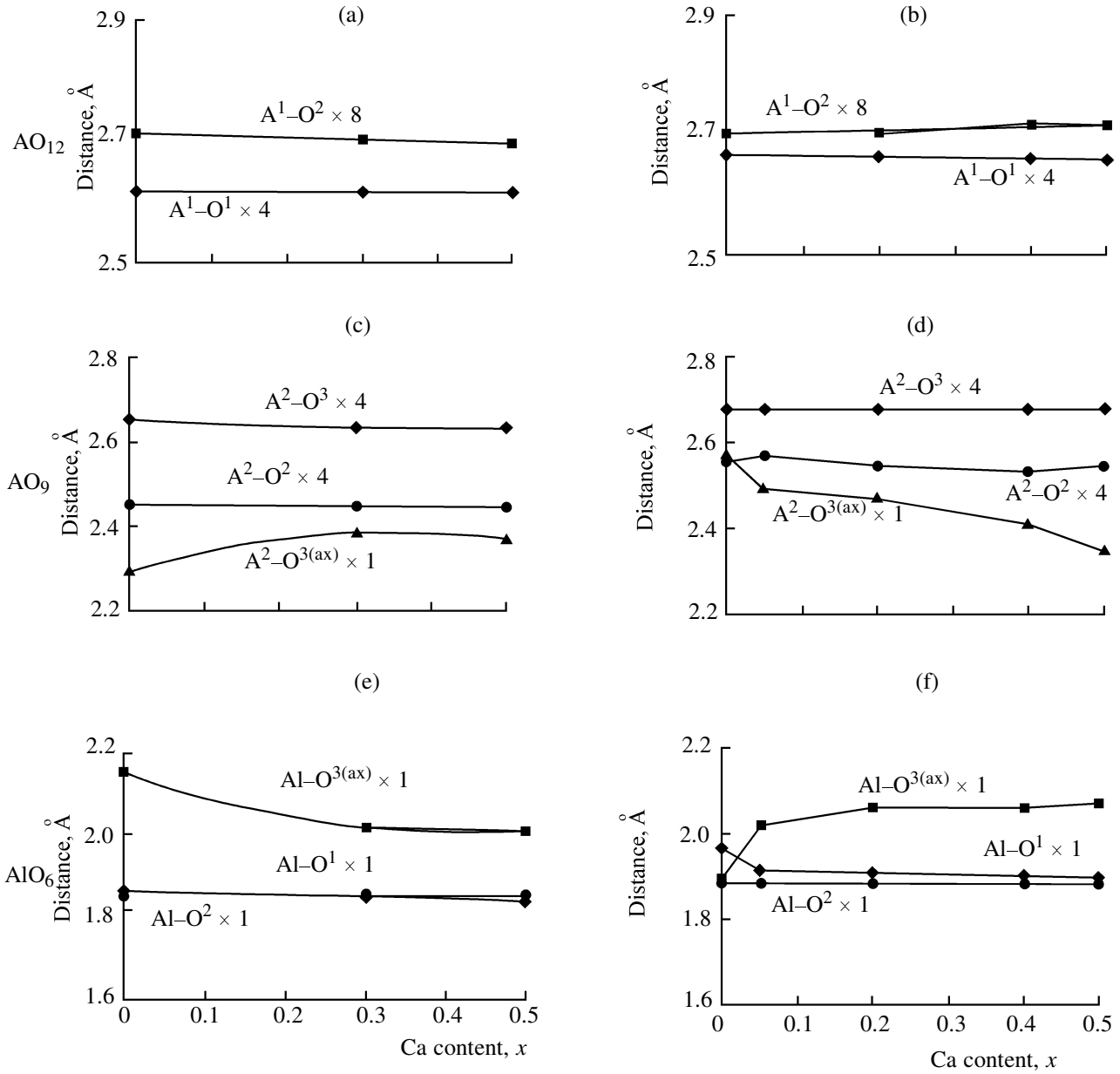

Fig. 4. Interatomic distances in AO_{12}, AO_9, and AlO_6 coordination polyhedra in solid solutions (a, c, e) $Gd_2Sr_{1-x}Ca_xAl_2O_7$ and (b, d, f) $La_2Sr_{1-x}Ca_xAl_2O_7$ as functions of the calcium content.

arranged in antiprisms than in the neodymium-containing solution. It agrees with the results of structural calculations of the polyhedron occupancies and is indicative of practically exclusive localization of Ca^{2+} in AO_9. The elongation of the $A–O^3$ bond length in a solid solution with gadolinium seems to be due to displacement of Gd^{3+} from the antiprisms by larger Ca^{2+}.

Significant anisotropy of interatomic interactions of aluminum with axial oxygen atoms ($Al–O^1$ and $Al–O^3$) is observed in AlO_6 oxygen octahedra forming double layers perpendicular to the *c*-axis of the structure, whereas the $Al–O^1$ and $Al–O^2$ bond lenths are practically equal both in $Gd_2SrAl_2O_7$ and in $Gd_2Sr_{1-x}\cdot Ca_xAl_2O_7$ solid solutions. Furthermore, aluminum atoms are shifted from the plane of equatorial oxygen atoms in the direction toward the axial O^1 atom, as indicated by differences in *z* coordinates for the Al and O^2 atoms (Table 2).

For $La_2SrAl_2O_7$, $Nd_2SrAl_2O_7$, and $Gd_2SrAl_2O_7$, the character of distortion of the octahedra is different. It is seen from Fig. 4 that, in $La_2SrAl_2O_7$, axial $Al–O^1$

bonds directed inside the perovskite layer are longer than the Al–O^3 bonds binding the perovskite and rock salt layers. In $Nd_2SrAl_2O_7$ and $Gd_2SrAl_2O_7$, the interatomic distances Al–O^3, on the contrary, are longer than Al–O^1. This difference increases in going to $La_2Sr_{0.5}Ca_{0.5}Al_2O_7$, $Nd_2Sr_{0.5}Ca_{0.5}Al_2O_7$, and $Gd_2Sr_{0.5}Ca_{0.5}Al_2O_7$ solid solutions despite smaller size of calcium ion compared to strontium: the Al–O^3 interatomic distance increases from 1.90 to 2.07 Å in the first case, from 2.04 to 2.06 Å in the second, and decreases from 2.15 to 2.01 Å in the third case. The length of equatorial Al–O^2 bonds remains in this case practically unchanged.

The distance A–O^3–Al between the perovskite and rock salt layers decreases in all the solid solutions (with simultaneous elongation of the Al–O^3 and shortening of A–O^3 axial bonds for lanthanum- and neodymium-containing solutions, and the inverse trend for the solid solution with gadolinium). At the same time, the thickness of the double perovskite layer *PP* (O^3–Al–O^1–Al–O^3) decreases in the gadolinium- and neodymium-containing solutions, but increases in the lanthanum-containing solution. This trend agrees with preferential occupation of the AO_{12} polyhedra in $La_2Sr_{0.5}Ca_{0.5}Al_2O_7$ by larger strontium cations, but does not agree with the data on the complete ordering of Sr^{2+} cations in the perovskite layer in $Gd_2Sr_{0.5}Ca_{0.5}Al_2O_7$. This effect may be due to an increase in the occupation of AO_{12} cuboctahedra by small Gd^{3+} cations in the $Gd_2Sr_{1-x}Ca_xAl_2O_7$ solutions (or Nd_{3+} cations in the $Nd_2Sr_{1-x}Ca_xAl_2O_7$ solutions) as the strontium content decreases. The competition of bonds in the (A–O^3–Al) chain connecting perovskite and rock salt layers is manifested in weakening of one bond (A–O^3) accompanied by strengthening of the other bond (Al–O^3). All these trends indicate that, as calcium cations are introduced into the matrix, the cation-oxygen bonds are strengthened within the limits of the perovskite layer and the interlayer bond weakens, destabilizing the layered structure as a whole.

In pure oxides $Ln_2SrAl_2O_7$, positional ordering reduces the probability of the composition fluctuations resulting in the formation of local areas in a perovskite layer enriched in rare-earth cations. Such areas can be precursors of the perovskite phase separation and can promote destabilization of the *PP–RS* layered structure, as demonstrated previously by the example of metastable oxide $LaCaAlO_4$ [13, 14]. For example, in $Nd_2SrAl_2O_7$ and $Gd_2SrAl_2O_7$ the enrichment of a rock salt layer in neodymium and gadolinium cations stabilizes the layer structure.

As the calcium content in $Ln_2Sr_{1-x}Ca_xAl_2O_7$ solid solutions increases, cations of rare-earth and alkaline-earth elements are redistributed between various layers of the structure. In lanthanum- and gadolinium-containing solutions, a discrepant pattern is observed: practically full occupation of the rock salt layer in $La_2Sr_{1-x}Ca_xAl_2O_7$ by calcium cations and full ordering of strontium cations in the perovskite layer in $Gd_2Sr_{1-x}Ca_xAl_2O_7$. In this case, the introduction of calcium cations into $Gd_2Sr_{1-x}Ca_xAl_2O_7$ and $Nd_2Sr_{1-x}Ca_xAl_2O_7$ solutions results in the displacement of rare-earth cations from *RS* layers, whereas the stabilizing role of positional ordering of cations with different charges weakens. This fact explains why the area of the existence of $Gd_2Sr_{1-x}Ca_xAl_2O_7$ and $Nd_2Sr_{1-x}Ca_xAl_2O_7$ solid solutions is not expanded as compared to $La_2Sr_{1-x}Ca_xAl_2O_7$.

Thus, the study of the $Ca^{2+} \rightarrow Sr^{2+}$ substitution in $Ln_2SrAl_2O_7$ matrices shows that the character and extent of ordering of cations can affect both the stability of the layered structure and the limits of the existence of solid solutions.

EXPERIMENTAL

Solid solutions $Gd_2Sr_{1-x}Ca_xAl_2O_7$ were synthesized by a ceramic method from gadolinium and aluminum oxides and strontium and calcium carbonates taken in proportions corresponding to Eq. (1).

$$Gd_2O^3 + Al_2O^3 + (1 - x)SrCO^3 + xCaCO^3 = Gd_2Sr_{1-x}Ca_xAl_2O_7 + CO^2. \quad (1)$$

The carefully mixed charge was pelletized and calcined at 1500°C in a Silit furnace in corundum crucibles in air. The phase composition of the calcined specimens was checked by X-ray diffraction on a DRON-3 diffractometer (in the range of 2θ angles 25°–100°) in CuK_α radiation. Phases were identified using the program complex DIFFRAC-AT (Version 3.1).

The X-ray patterns for structural calculations were taken on a Philips PW 200 analytical X-ray system within the range of 2θ angles from 5° to 110° at 0.04° steps and a constant counting time of 12 s. The unit cell parameters, atomic coordinates, and interatomic distances were determined in space group *I*4/*mmm* from the full profile of X-ray patterns with subsequent refinement by Rietveld's method using the FULLPROF program [15, 16].

ACKNOWLEDGMENTS

This study was financially supported by the Russian Foundation for Basic Research (project no. 04-03-32176).

REFERENCES

1. Zvereva, I.A., Isaeva, A.S., and Choisnet, J., *Zh. Obshch. Khim.,* 2006, vol. 76, no. 6, p. 915.
2. Ohyama, T., Ohashi, N., Fukunaga, O., Ikawa, H., Izumi, F., and Tanaka, J., *Physica C,* 1995, vol. 249, p. 293.
3. Ngueyn Er-rakho, L., Michel, C., Choisnet, J., and Raveau, B., *Mater. Res. Bull.,* 1980, vol. 15, no. 5, p. 891.
4. Ganguly, R., Siruguri, V., Gopalakrishnan, I.K., and Yakhmi, J.V., *J. Phys.: Condens. Matter,* 2000, vol. 12, p. 1683.
5. Chang, C.F., Chou, P.H., Tsay, H.L., Weng, S.S., Chatterjee, S., and Yang, H.D., *Phys. Rev. (B),* 1998, vol. 58, no. 18, p. 12224.
6. Zvereva, I., Zueva, L., and Choisnet, J., *J. Mater. Sci.,* 1995, vol. 30, p. 3598.
7. Zvereva, I., Smirnov, Yu., and Choisnet, J., *Int. J. Inorg. Mater.,* 2001, vol. 3, no. 1, p. 95.
8. Zvereva, I.A., Seitablaeva, S.R., and Smirnov, Yu.E., *Zh. Obshch. Khim.,* 2003, vol. 73, no. 1, p. 35.
9. Ruddlesden, S.N. and Popper, P., *Acta Crystallogr.,* 1958, vol. 11, no. 1, p. 54.
10. Shannon, R.D., *Acta Crystallogr., Sect. A,* 1976, vol. 32, no. 5, p. 751.
11. Zvereva, I., Smirnov, Yu., Gusarov, V., Popova, V., and Choisnet, J., *Solid State Sci.,* 2003, vol. 5, no. 2, p. 343.
12. Cava, R.J., Siegrist, T., Peck, W.F.Yr., Kraewski, J.J., Battlog, B., and Rosamilia, J., *Phys. Rev., Ser. 3B,* 1978, vol. 18, p. 9746.
13. Smirnov, Yu., Zvereva, I., and Choisnet, J., *J. Solid State Chem.,* 1997, vol. 134, no. 1, p. 132.
14. Zvereva, I., Smirnov, Yu., and Choisnet, J., *Mater. Chem. Phys.,* 1999, vol. 60, no. 1, p. 63.
15. Rietveld, H., *Appl. Crystallogr.,* 1969, vol. 2, no. 1, p. 65.
16. Rodriguez-Carvajal, J.L., *Physica B,* 1992, vol. 192, no. 1, p. 55.